Report

Cell Reports

In Vivo Ca^{2+} Imaging Reveals that Decreased Dendritic Excitability Drives Startle Habituation

Graphical Abstract

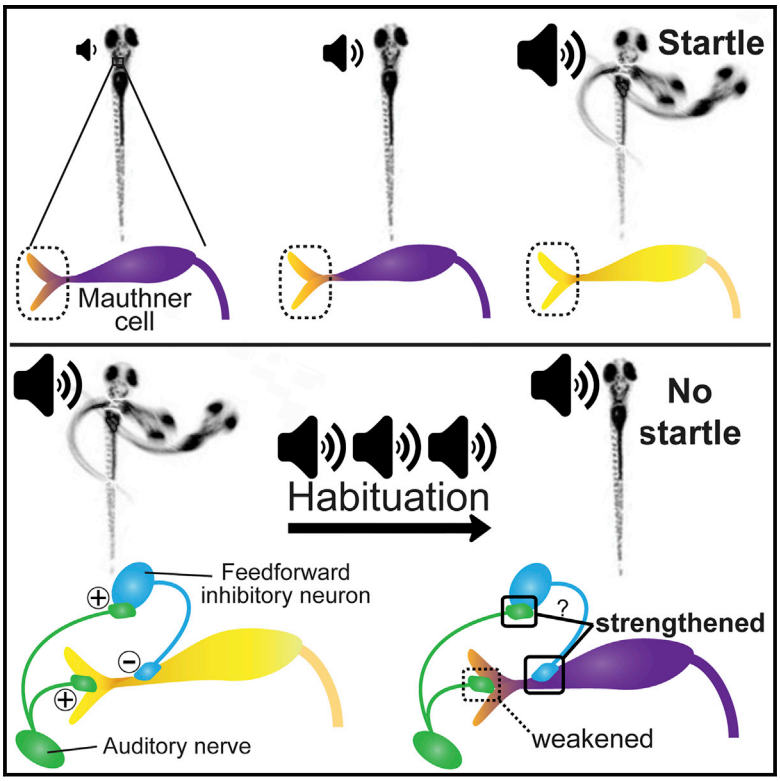

Authors

Kurt C. Marsden, Michael Granato

Correspondence

granatom@mail.med.upenn.edu

In Brief

The neuronal mechanisms that govern short-term habituation of the startle response are unclear. Using GCaMP6s to visualize subcellular activity in the zebrafish startle command neuron, the Mauthner cell, Marsden and Granato show that depression of dendritic excitability rather than downstream inhibition underlies short-term habituation.

Highlights

- GCaMP6s enables analysis of subcellular neuronal activity during startle behavior
- Startle regulation occurs both up- and downstream of the Mauthner cell
- Downstream inhibition does not play a role in short-term habituation
- Short-term habituation is due to depression of Mauthner cell dendritic excitability

Marsden & Granato, 2015, Cell Reports *13*, 1733–1740
December 1, 2015
http://dx.doi.org/10.1016/j.celrep.2015.10.060

CellPress

Cell Reports
Report

In Vivo Ca^{2+} Imaging Reveals that Decreased Dendritic Excitability Drives Startle Habituation

Kurt C. Marsden[1] and Michael Granato[1,*]
[1]Department of Cell and Developmental Biology, University of Pennsylvania Perelman School of Medicine, Philadelphia, PA 19104, USA
*Correspondence: granatom@mail.med.upenn.edu
http://dx.doi.org/10.1016/j.celrep.2015.10.060

SUMMARY

Exposure to repetitive startling stimuli induces habituation, a simple form of learning. Despite its simplicity, the precise cellular mechanisms by which repeated stimulation converts a robust behavioral response to behavioral indifference are unclear. Here, we use head-restrained zebrafish larvae to monitor subcellular Ca^{2+} dynamics in Mauthner neurons, the startle command neurons, during startle habituation in vivo. Using the Ca^{2+} reporter GCaMP6s, we find that the amplitude of Ca^{2+} signals in the lateral dendrite of the Mauthner neuron determines startle probability and that depression of this dendritic activity rather than downstream inhibition mediates glycine and N-methyl-D-aspartate (NMDA)-receptor-dependent short-term habituation. Combined, our results suggest a model for habituation learning in which increased inhibitory drive from feedforward inhibitory neurons combined with decreased excitatory input from auditory afferents decreases dendritic and Mauthner neuron excitability.

INTRODUCTION

To efficiently navigate their environments, animals filter sensory information such that they attend to salient stimuli while ignoring irrelevant ones. This task requires the nervous system to establish and modify behavioral thresholds to ensure that the behavioral response to a stimulus is appropriate to the environmental context. A prime example of this is habituation, a non-associative form of learning (Thompson and Spencer, 1966) in which repeated inconsequential stimuli elicit a progressive decline in the behavioral response (Groves and Thompson, 1970; Rankin et al., 2009; Thompson and Spencer, 1966). Deficits in habituation are observed in complex brain disorders including schizophrenia (Meincke et al., 2004; Swerdlow et al., 2006) and autism (Dinstein et al., 2012; Kleinhans et al., 2009), yet the neural circuit mechanisms that mediate this behavioral plasticity remain unclear.

Habituation of the acoustic startle response is well documented in mammals and fish, and it displays similar neuropharmacological modulation in both groups (Carey et al., 1998; Halberstadt and Geyer, 2009; Wolman et al., 2011), suggesting that key mechanisms underlying habituation are evolutionarily conserved. In both adult goldfish and larval zebrafish, a single pair of bilateral reticulospinal neurons, the Mauthner cells (M-cells), serve as the so-called command neurons of the startle response (Korn and Faber, 2005), as they are active only during these fast startle responses and without them fast startle behaviors are abolished (Burgess and Granato, 2007; Satou et al., 2009). Moreover, several studies have implicated M-cells and giant neurons in the mammalian reticular formation, the functional equivalent of the M-cell system, in startle habituation (Aljure et al., 1980; Roberts et al., 2011; Simons-Weidenmaier et al., 2006; Weber et al., 2002), indicating that regulation of M-cell activity is likely to be central to startle modulation such as habituation learning.

RESULTS

To study circuit dynamics during acoustic startle habituation, we established a method to simultaneously monitor startle circuit activity and behavior in 5-day post-fertilization (dpf) zebrafish larvae. The larval zebrafish startle circuit is simple and accessible, with hair cells in the otic vesicle stimulating eighth (VIII) nerve fibers that directly activate the M-cell at mixed chemical and electrical synapses (Yao et al., 2014). The M-cell then triggers contralateral spinal motor neurons to contract body wall muscle to initiate the stereotyped C-bend response (Figure 1A). To assess M-cell activity, we generated a *UAS:GCaMP6s* transgenic line and crossed these fish with the *Gal4FF-62A* line that selectively labels the M-cells (Yamanaka et al., 2013) to optically isolate GCaMP6s-labeled M-cells. Similar to previous studies (O'Malley et al., 1996; Takahashi et al., 2002), transgenic larvae were individually mounted in glass-bottom petri dishes and partially restrained in agarose such that their heads were fixed but their tails were free to move. Tail movements were captured at 500 Hz with a high-speed camera mounted above the stage of a spinning disc confocal microscope. Acoustic-vibrational stimuli were delivered via a small speaker connected to the microscope stage. This non-directional stimulus was calibrated to elicit startle responses to >90% of stimuli while inducing minimal movement of the sample. Larvae were each given 10–11 such stimuli (13 dB) with a minimum of 2 min between stimuli to minimize habituation. Of the 155 total stimuli we observed 7 no-responses (4.5%), while the majority of stimuli resulted in startle responses that could be distinguished by latency. The vast majority of startles (n = 137, 88.4% of stimuli) initiated between 4 and 10 ms (short-latency C-bends [SLCs]; Figures 1B and 1C), while the remainder (n = 11, 7.1%) initiated between 14 and

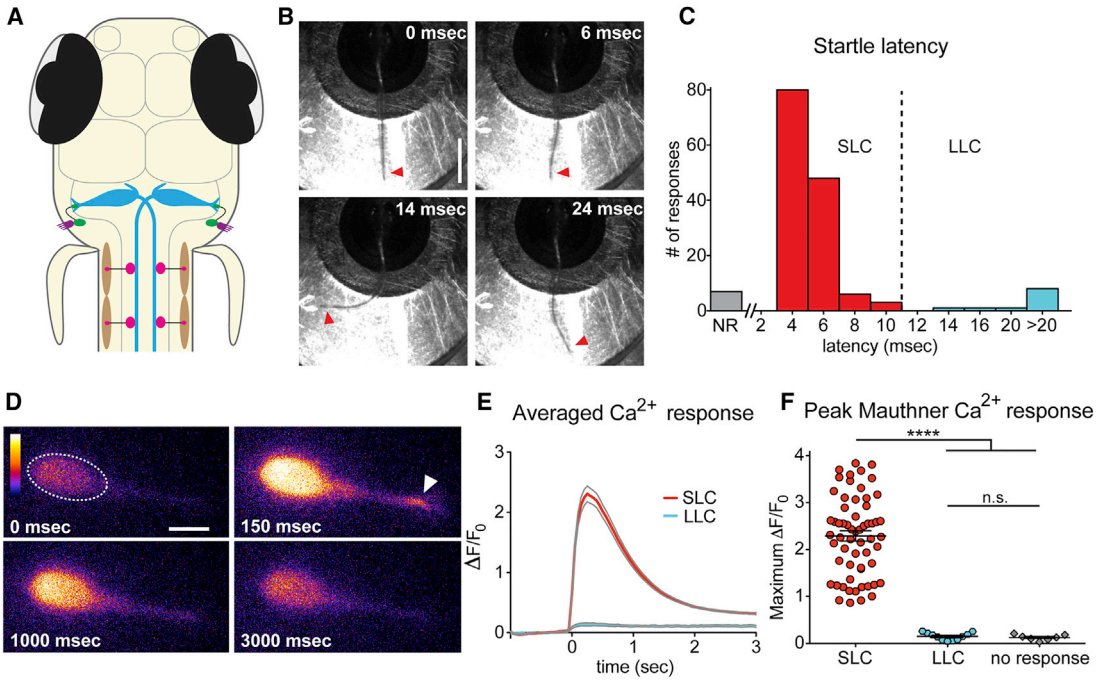

Figure 1. The Mauthner Cell Is Active Only during Short-Latency C-Bends and Not during Long-Latency C-Bends

(A) The larval zebrafish acoustic startle circuit: hair cells in the otic vesicle (purple), VIII nerve afferents (green), hindbrain Mauthner cells (M-cells, blue), spinal motor neurons (pink), and contraction of muscle (brown).

(B) High-speed images (500 Hz) of a short-latency C-bend (SLC) in a head-restrained 5-dpf larva. Arrowheads highlight tail (scale bar, 1 mm).

(C) Distribution of startle latencies in head-restrained larvae (NR, no response; LLC, long-latency C-bend).

(D) Representative example of M-cell activation following acoustic stimulation in a *Gal4FF62a;UAS:GCaMP6s* transgenic larva. Arrowhead highlights lateral dendrite activation. Color scale denotes fluorescence intensity (black, lowest; white, highest; scale bar, 10 μm).

(E) Averaged traces show change in fluorescence (ΔF) relative to baseline (F_0) for SLC (red) and LLC (blue) responses performed to the contralateral side of the imaged M-cell. Gray lines indicate SEM.

(F) Scatterplot of peak $\Delta F/F_0$ values for contralateral SLCs, LLCs, and NRs. (****$p < 0.0001$, t test). Error bars indicate SEM.

46 ms (long-latency C-bends [LLCs]; Figure 1C). There was no significant bias in the direction of the behavioral response, with roughly equal numbers of tail flips to the left (n = 77) and right (n = 60). These data are similar to previous data from free-swimming larvae (Burgess and Granato, 2007), and thus this preparation and the GCaMP6s transgene do not significantly affect larval startle behaviors.

To achieve optimal spatial and temporal resolution, we imaged individual M-cells at 63X magnification and captured a single confocal plane at 20 Hz. During SLCs in which the tail turned contralateral to the imaged M-cell we observed robust Ca^{2+} signals in the M-cell soma, consistent with an M-cell action potential (n = 60; mean $\Delta F/F_0$: 2.29 ± 0.11; Figures 1D–1F). The kinetics of these Ca^{2+} spikes (rise time: 197 ± 4 ms; decay time: 803 ± 20 ms) were similar to those observed using GCaMP6s during a single action potential in mouse visual cortical neurons (Chen et al., 2013). In contrast, we saw very little to no change in GCaMP6s fluorescence during LLCs (n = 11; mean $\Delta F/F_0$: 0.15 ± 0.02; Figures 1E and 1F), regardless of whether the response was contralateral or ipsilateral to the M-cell being imaged. LLC Ca^{2+} signals were indistinguishable from those observed when there was no behavioral response (mean $\Delta F/F_0$: 0.13 ± 0.02, p = 0.5133; Figure 1F), supporting previous data showing that M-cells are active only during fast startle responses (Kohashi and Oda, 2008) and are dispensable for LLCs but required for SLCs (Burgess and Granato, 2007; Satou et al., 2009), which hereafter we will refer to as "startles." Furthermore, imaging of M-cell Ca^{2+} responses has shown that these signals rely exclusively on Ca^{2+} influx through voltage-gated channels rather than release from internal stores (Takahashi et al., 2002). Thus, GCaMP6s imaging provides an accurate reflection of M-cell membrane potential and activation state.

During our analysis of M-cell Ca^{2+} responses, we frequently observed changes in fluorescence at the lateral dendrite (Figure 1D, arrowhead), the site of synaptic input from VIII sensory afferents. To determine whether these signals represent subthreshold postsynaptic responses, we presented a series of acoustic stimuli of increasing intensity (−24 to 13 dB) and monitored the M-cell lateral dendrite for changes in Ca^{2+}. We detected activation of the lateral dendrite in the absence of somatic activation even at very low stimulus intensities (Figures 2A–2C; Movie S1). Specifically, levels of lateral dendrite activity increased as the intensity of the stimulus increased, while somatic activity was negligible unless the larvae performed a startle (n = 270 stimuli in 15 fish; Figure 2C). These data suggest that lateral dendrite Ca^{2+} signals represent graded postsynaptic

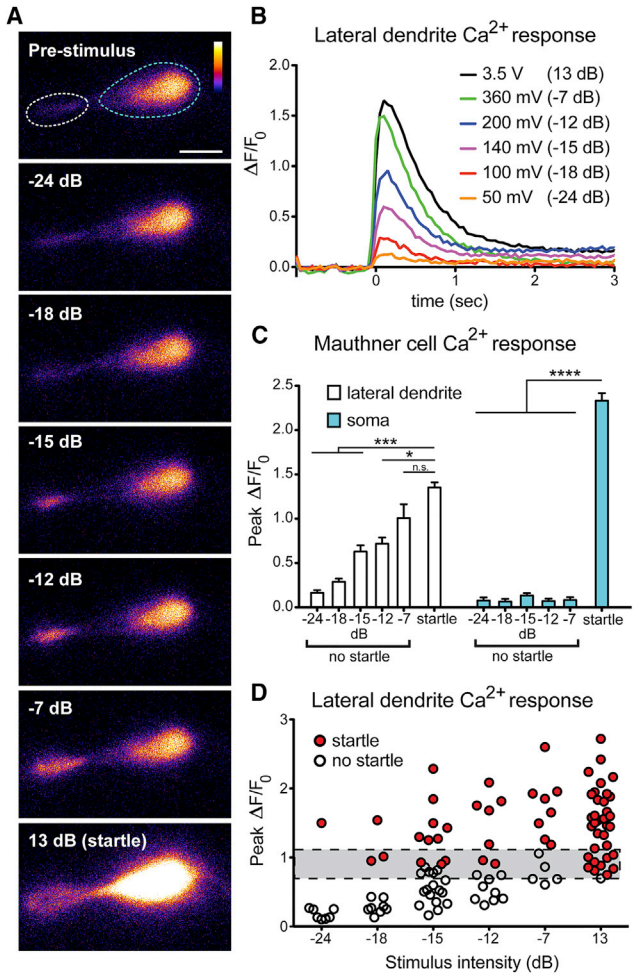

Figure 2. Graded M-Cell Lateral Dendrite Ca^{2+} Signals Reflect Startle Probability

(A) Increasing stimulus intensity increases activity at the M-cell lateral dendrite (white dashed line), with no change in somatic (blue dashed line) activity unless a startle is performed (scale bar, 10 μm).

(B) Representative $\Delta F/F_0$ traces from a single M-cell show graded lateral dendrite responses. Stimuli were calibrated with an accelerometer, with voltage outputs converted to dB using the formula dB = 20 log (V/0.775).

(C) Grouped $\Delta F/F_0$ data reveal all-or-none somatic activity (blue bars) in startles versus non-startles regardless of stimulus intensity and graded lateral dendrite activity (white bars; *p < 0.05, ***p < 0.001, ****p < 0.0001, one-way ANOVA with Dunnett's multiple comparison test). Error bars indicate SEM.

(D) Scatterplot of peak lateral dendrite $\Delta F/F_0$ with startle events in red and no startle events in white. Gray bar indicates the lateral dendrite activation threshold for startle behavior.

potentials while somatic Ca^{2+} responses indicate all-or-nothing action potentials. Moreover, a scatterplot of the same lateral dendrite Ca^{2+} responses reveals the level of activity required for startle behavior and that the amplitude of lateral dendrite activation determines the startle probability (Figure 2D), suggesting that plasticity of these dendritic responses may be involved in startle threshold modulation during habituation.

In free-swimming larvae, repeated strong acoustic stimulation rapidly induces habituation (Wolman et al., 2011). We tested head-restrained larvae in this simple learning task with 30 stimuli at 13 dB, the first 5 with a 2 min inter-stimulus interval (ISI) and the final 25 stimuli with a 5 s ISI. We observed robust habituation, as startle frequency decreased from 0.97 ± 0.03 to 0.19 ± 0.04 (n = 19 larvae; Figure 3A). One possible mechanism for this behavioral plasticity is that inhibition downstream of the M-cell prevents motor neuron activation. Earlier work has shown that acoustic stimulation can activate both M-cells but that a set of spinal inhibitory neurons downstream of the M-cell, CoLos, prevent the trailing spike from activating motor neurons, ensuring a unilateral behavioral response (Satou et al., 2009). To confirm that inhibition downstream of the M-cell is operational in our system, we imaged both M-cells at 40× magnification in five larvae and observed that 29/50 (58%) stimuli at 13 dB elicited bilateral M-cell activation, with the remaining 42% triggering unilateral M-cell responses (Figure 3B). Similarly, when we imaged one M-cell at 63× and analyzed only startle events toward the ipsilateral side of the recorded M-cell, the majority of such events (56/85; 66%) were associated with robust M-cell responses (mean $\Delta F/F_0$: 2.58 ± 0.12) indistinguishable from those during contralateral startles (Figure 1F). In the remaining 29/85 (33%) ipsilateral startles M-cell activation was negligible (mean $\Delta F/F_0$: 0.14 ± 0.01). These data demonstrate a strong and reliable source of inhibition downstream of the M-cell soma, consistent with the idea that this mechanism is engaged during habituation.

This model predicts that during habituation the M-cell soma continues to be activated but that this is insufficient to trigger startle behavior. To test this prediction we analyzed M-cell Ca^{2+} responses during our 30-stimulus habituation protocol. Contrary to the model, however, the frequency of somatic Ca^{2+} responses, likely representing all-or-nothing action potentials (Figure 2C), followed the behavioral output and decreased rapidly (0.96 ± 0.02 to 0.14 ± 0.06; n = 19 fish; Figures 3C and 3D). To directly test whether CoLo inhibitory interneurons are dispensable for startle habituation, we bilaterally laser-ablated all CoLos caudal to the fifth segment at 2–2.5 dpf using the Tol056 transgenic line that labels CoLos and M-cells with GFP (Satou et al., 2009). Ablations were confirmed by imaging 24 hr post-ablation (Figure 3E). At 5 dpf, CoLo-ablated larvae showed no difference in startle habituation compared to non-ablated controls when tested in a free-swimming version of the same 30-stimulus assay (control: n = 17; CoLo-ablated n = 4; Figure 3F). Importantly, startle responses in CoLo-ablated larvae were abnormal in that the tail straightened and shortened (Figure S1A), indicative of bilateral muscle contraction due to the elimination of inhibition that prevents bilateral M-cell activation (Satou et al., 2009). These data provide compelling evidence against a habituation mechanism requiring inhibition downstream of the M-cell soma.

A second possible mechanism is that depression of M-cell lateral dendrite responses prevents M-cell activation during habituation. To measure whether changes in lateral dendrite activity are associated with habituation, we compared activity in habituated and non-habituated larvae. We and others have previously identified the N-methyl-D-aspartate (NMDA) receptor inhibitor MK-801 as a potent inhibitor of short-term habituation in 5 dpf zebrafish (Roberts et al., 2011; Wolman et al., 2011), and we also tested the role of glycinergic inhibition during habituation using

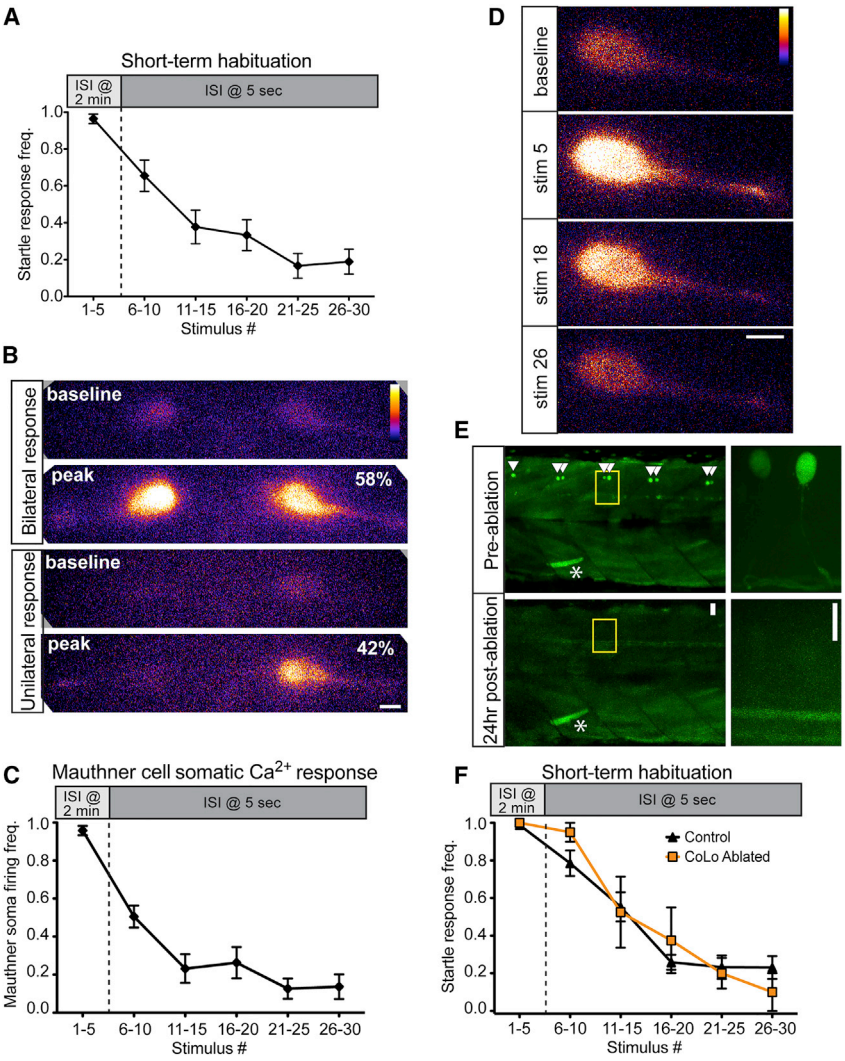

Figure 3. Inhibition Downstream of the M-Cell Does Not Cause Startle Habituation

(A) A 30-stimulus assay (5 pulses at 2 min ISI and 25 pulses at 5 s ISI) induced robust startle habituation in head-restrained larvae. Error bars indicate SEM.

(B) 40× magnification images of bilateral M-cell GCaMP6s labeling demonstrate unilateral (bottom, 42%) and bilateral (top, 58%) M-cell firing (n = 50 responses from five fish; scale bar, 10 μm).

(C) The frequency of M-cell somatic Ca^{2+} responses during short-term habituation is strongly reduced during habituation. Error bars indicate SEM.

(D) Representative images show baseline and peak fluorescence for non-habituating (stim 5) and habituating stimuli (stim 18 and 26; scale bar, 10 μm).

(E) Representative images at 10× (left) and 63× (right) show pre-ablation labeling of CoLo interneurons and their absence 24 hr post-ablation. Asterisk highlights a GFP-labeled muscle cell to indicate the same segments are imaged pre- and post-ablation (scale bar 10 μm).

(F) Both control and CoLo-ablated larvae rapidly habituate to repeated acoustic stimulation. Error bars indicate SEM.

the glycine receptor blocker strychnine. A 15-min application of MK-801 (500 μM) or strychnine (100 μM) prior to testing dramatically reduced habituation (MK801: 1.0 ± 0.0 to 0.78 ± 0.08, n = 8; strychnine: 1.0 ± 0.0 to 0.91 ± 0.09, n = 9) compared to DMSO-treated larvae (1.0 ± 0.0 to 0.20 ± 0.05; n = 8; Figure 4A). After 5 min rest, we gave one more stimulus, and startle responsiveness spontaneously recovered (Figure 4A). These data demonstrate that while CoLo-mediated inhibition downstream of the M-cell is dispensable, other populations of glycinergic neurons are essential for startle habituation. MK-801 treatment did not alter M-cell GCaMP6s properties, as peak fluorescence (Figure 4B) and kinetics (Figure 4C) of Ca^{2+} signals were unchanged. Thus, NMDA receptors contribute minimal Ca^{2+} to GCaMP6s signals in the M-cell. Strychnine caused bilateral muscle contraction (Figure S1B) and also increased the amplitude and decay time of lateral dendrite and somatic Ca^{2+} signals (Figures 4B and 4C), indicating that glycinergic inhibition shapes M-cell activity.

Next, we measured M-cell activity during habituation. In untreated larvae, we consistently observed decreases in peak GCaMP6s fluorescence associated with startle responses and M-cell somatic activation during the habituation protocol (Figure 3D, stim 5 versus stim 18). Ca^{2+} responses during action potential-like events in which there was a startle response *and* a strong Ca^{2+} signal in the M-cell soma (>10 SDs above signals when there was no startle response) were significantly decreased (soma: 58.9% ± 2.84%; lateral dendrite: 79.3% ± 1.44%; n = 26 larvae; Figures S2A and S2B). This effect is largely independent of the effects of illumination, as peak $\Delta F/F_0$ decreased only slightly when the imaging laser was on for the same duration as the habituation assay but no acoustic stimuli were delivered (soma: 0.13% ± 6.45%, lateral dendrite: 14.8% ± 6.41%; n = 9; Figures S2C and S2D). Because M-cell soma and lateral dendrite responses did not change when all 30 stimuli were separated by 2 min (Figures S2E and S2F), the decrease in action potential signals during habituation is likely due to repeated excitation of GCaMP6s. Because of the high affinity of GCaMP6s for Ca^{2+}, repeated stimulation would reduce GCaMP6s sensitivity, a phenomenon observed with other Ca^{2+} indicators (Takahashi et al., 2002). Critically, Ca^{2+} signals remained robustly detectable above noise.

Lateral dendrite Ca^{2+} responses during habituation were normalized to the curve in Figure S2B. In strongly habituated, DMSO-treated larvae, these signals were decreased by ~35%, while in non-habituated, MK-801-treated larvae, no significant depression was observed (DMSO: n = 8; MK-801: n = 8; $p < 0.0001$, two-way ANOVA; Figure 4D). Lateral dendrite signals recovered to baseline after a 5-min rest. Finally, lateral dendrite signals in non-habituated strychnine-treated larvae were decreased from their baseline but remained elevated relative to DMSO controls (strychnine: n = 6; $p < 0.0001$, two-way

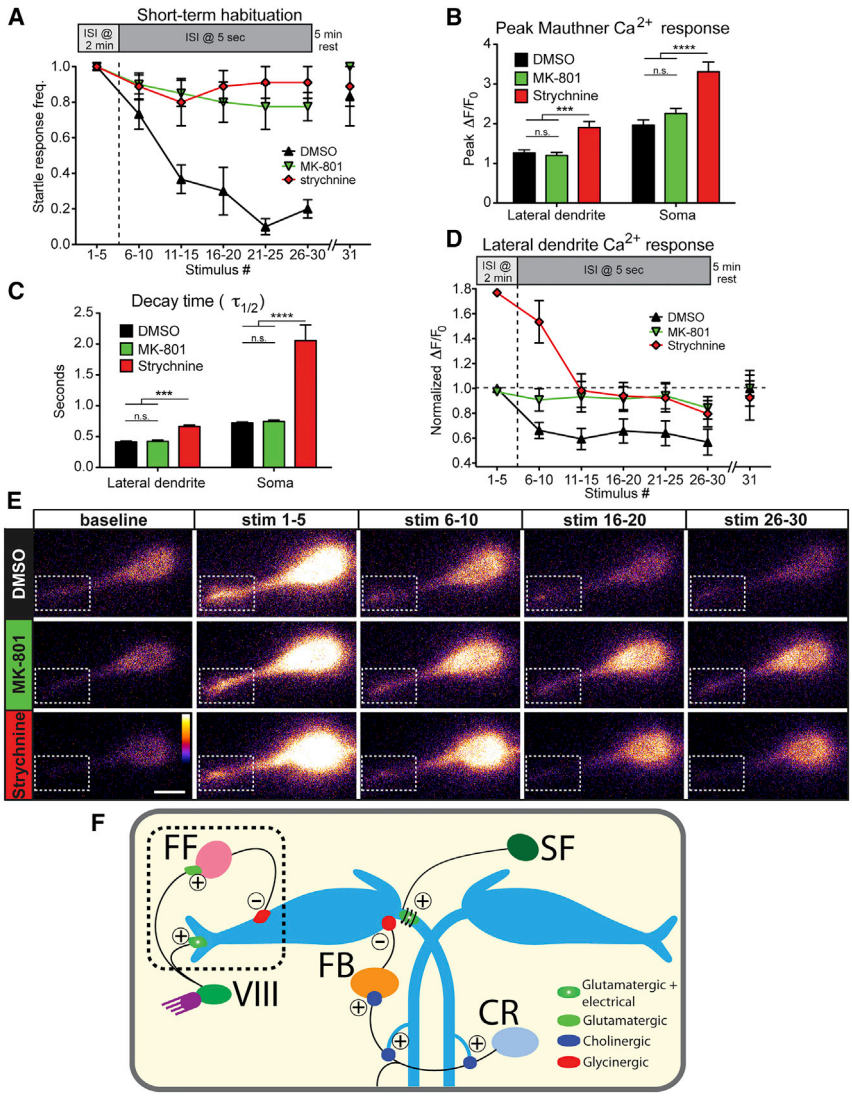

Figure 4. PSP Depression Drives Short-Term Startle Habituation

(A) 500 μM MK-801 (n = 8) and 100 μM strychnine (n = 9) strongly reduce short-term habituation of the startle response compared to DMSO-treated controls (n = 8). A 5-min rest period allows complete recovery to the 31st stimulus.

(B) Peak $\Delta F/F_0$ levels in M-cell lateral dendrite and soma are unaffected by MK-801 but are increased by strychnine (***p < 0.001, ****p < 0.0001, t test).

(C) Ca^{2+} signal decay kinetics are unaltered by MK-801 but are increased by strychnine (***p < 0.001, ****p < 0.0001, t test).

(D) Normalized M-cell lateral dendrite Ca^{2+} responses are decreased ~35% in DMSO-treated fish during habituation while MK-801 treatment prevented this decrease (****p < 0.0001, two-way ANOVA). Responses in strychnine-treated larvae decreased from a higher baseline but remained elevated compared DMSO-treated larvae (****p < 0.0001, two-way ANOVA).

(E) Representative images for each block of five stimuli show PSP depression in DMSO compared to MK-801- and strychnine-treated fish. Dashed box highlights lateral dendrite (scale bar, 10 μm).

(F) Diagram of the M-cell circuit including known regulatory inputs. Startle habituation arises from an NMDA- and glycine-receptor dependent mechanism that likely results in enhanced transmission from feedforward (FF) inhibitory neurons to the M-cell and may involve depression of acoustic nerve (VIII) inputs to the M-cell. Inputs from downstream spiral fiber (SF), cranial relay (CR), and feedback inhibitory (FB) neurons are most likely not involved in startle habituation. Excitatory (+) and inhibitory (–) connections are labeled.

In (A)–(D), error bars indicate SEM.

ANOVA; Figure 4D). These data indicate that habituation results from an NMDA- and glycine-receptor-dependent decrease in dendritic excitability below a critical threshold.

Repetitive stimuli at different ISIs can engage different mechanisms to produce habituation (Broster and Rankin, 1994; Wicks and Rankin, 1996). To test whether depression of lateral dendrite activity is a general mechanism for larval zebrafish startle habituation, we doubled the ISI to 10 s. As before, DMSO-treated larvae strongly habituated, but more slowly (Wolman et al., 2011), while MK-801-treated larvae showed very little habituation (Figure S3A). Similar to the 5-s ISI assay, lateral dendrite signals decreased ~35% in DMSO controls, while MK-801-treated larvae showed no change in dendritic activity (DMSO: n = 6; MK-801: n = 8; p < 0.0001; Figure S3B). Startle behavior and dendritic activity recovered for both groups following the rest period. These data illustrate the plasticity of the startle circuit and reveal a general mechanism for startle habituation: depression of M-cell lateral dendrite excitability.

DISCUSSION

Behavioral plasticity such as learning is characterized by changes in neuronal activity (Bliss and Lomo, 1973; Castellucci and Kandel, 1974). While these changes are often thought to be input-specific and limited to a subset of synapses on a given neuron (Harvey and Svoboda, 2007; Hebb, 1964; Wen and Barth, 2011), how such subcellular modulation of activity regulates behavioral output is difficult to assess in behaving animals. In this study we utilize a non-invasive optical approach to record changes in subcellular neuronal activity in a behaving vertebrate during a simple learning task. Using this approach, we identify the M-cell lateral dendrite as the site of startle threshold regulation and demonstrate that depression of dendritic excitability drives habituation learning.

Advances in Ca^{2+} indicators and microscopy have increased our understanding of the neuronal mechanisms of some forms of learning (Ahrens et al., 2012; Cichon and Gan, 2015), although

in vivo evidence for the mechanisms underlying vertebrate startle habituation is incomplete. Habituation of the *Aplysia* tactile gill and siphon withdrawal reflex appears to be driven by homosynaptic depression at the sensorimotor synapse (Glanzman, 2009). Similarly, work in hatchet fish suggests that acoustic startle habituation could result from decreased synaptic transmission at the VIII-M-cell synapse (Aljure et al., 1980). Supporting this mechanism, in vitro data from rat brain slices suggest that presynaptic depression at axon terminals of sensory afferents onto giant caudal pontine reticular nucleus (PnC) neurons, the mammalian analogs of the M-cells, might underlie short-term startle habituation (Simons-Weidenmaier et al., 2006; Weber et al., 2002). Recent data from larval zebrafish show that increasing electrical stimulation of auditory hair cells triggers stepwise increases in M-cell excitatory postsynaptic potentials (EPSPs), indicating recruitment of additional sensory afferents and activation of more club endings on the M-cell (Yao et al., 2014). Our subthreshold Ca^{2+} imaging data (Figure 2) reflect this pattern, so this is likely part of the mechanism for the graded dendritic responses we observe with increased acoustic stimulation. Depression of these same inputs thus might be involved in the dendritic depression we observe during habituation (Figure 4D). Because dendritic signals still undergo depression in the presence of strychnine, which prevents habituation (Figures 4A and 4D), depression of dendritic excitability is independent of inhibition but is not sufficient to induce habituation. We cannot exclude, however, that when all glycine receptors are blocked changes at sites other than the lateral dendrite may also contribute to startle habituation.

An alternative mechanism for habituation has been proposed based on data from multiple systems. Potentiation of inhibitory synapses is implicated in habituation of the *Aplysia* siphon withdrawal reflex (Bristol and Carew, 2005; Fischer et al., 1997), the crayfish escape response (Krasne and Teshiba, 1995; Shirinyan et al., 2006), and the *Drosophila* proboscis extension response to sweet stimulation (Paranjpe et al., 2012). Similarly, decreased startle responsiveness during a conditioning program similar to habituation is mediated by inhibitory long-term potentiation (iLTP) in the adult goldfish M-cell (Oda et al., 1998).

Three sources of inhibition in the larval zebrafish startle circuit have been identified: (1) CoLos, spinal interneurons activated by M-cell axons that inhibit motor neurons (Satou et al., 2009); (2) glycinergic feedback (FB) inhibitory neurons, which are activated by M-cell firing via cranial relay neurons (CRNs) and inhibit the M-cell at its axon cap (Koyama et al., 2011; Takahashi et al., 2002); and (3) glycinergic feedforward (FF) inhibitory neurons, often called passive hyperpolarizing potential (PHP) neurons (Koyama et al., 2011). Our analysis directly rules out CoLos from the habituation mechanism (Figure 3F), and our data implicating both NMDA receptors and glycine receptors (Figures 4A and 4D) are inconsistent with a CRN-FB pathway, as this is a cholinergic connection (Koyama et al., 2011). Inhibitory drive from these neurons is also inconsistent with the absence of M-cell somatic activity and depression of lateral dendrite activity we observe during startle habituation (Figures 3 and 4). Excitatory spiral fiber (SF) neurons, recently implicated in regulating M-cell firing and startle probability (Lacoste et al., 2015) can likely be excluded on similar grounds as their input lies downstream of the M-cell soma. FF neurons, on the other hand, receive glutamatergic input from VIII afferents and are known to regulate the startle threshold in adult goldfish (Weiss et al., 2008) and African cichlid fish (Neumeister et al., 2010), and in larval zebrafish, these neurons are adjacent to the M-cell lateral dendrite (Koyama et al., 2011), where their input likely influences dendritic responses. Our data are consistent with work in adult goldfish showing that inhibitory synapses on the M-cell are potentiated by repeated stimulation through a partially NMDA-receptor-dependent pathway (Korn et al., 1992; Oda et al., 1998). Although we cannot rule out that changes in voltage-gated channels also contribute to dendritic depression during habituation, our data suggest a model in which repeated stimulation of VIII afferents with startling stimuli activates NMDA receptors on the M-cell, resulting in decreased excitatory transmission at these synapses. Simultaneously, activation of NMDA receptors on FF neurons, the M-cell or both produces a strengthening of FF-to-M-cell synapses, resulting in decreased dendritic excitability and reduced startle probability (Figure 4F). These changes in synaptic efficacy may take place through either pre- or post-synaptic mechanisms.

It is important to note that the acoustic startle response in zebrafish is all-or-none (Burgess and Granato, 2007; Kimmel et al., 1974). Thus, the habituation we describe here is a change in startle probability, not magnitude. Habituation of response probability and magnitude in *C. elegans* following tap stimulation have been demonstrated to rely on different mechanisms (Kindt et al., 2007), and so it will be interesting to test whether this holds true for habituation of other larval zebrafish behaviors that exhibit graded responses such as the O-bend response to changes in illumination (Wolman et al., 2014). The optical method we describe here provides a powerful, noninvasive technique for investigating changes in circuit activity in an intact, genetically tractable vertebrate organism during learning. Future investigations will be able to benefit from this approach using the large library of zebrafish Gal4 lines (Kawakami et al., 2010; Scott et al., 2007) and recently identified mutants with habituation defects (Wolman et al., 2015) to better understand the cellular and molecular program underlying this behavioral plasticity.

EXPERIMENTAL PROCEDURES

Generation and Maintenance of Zebrafish

UAS:GCaMP6s fish were generated in the Tüpfel longfin (TLF) strain with I-SceI-mediated transgenesis as described previously (Thermes et al., 2002). *Gal4FF-62A* fish were kindly provided by Koichi Kawakami (Yamanaka et al., 2013). Embryos were raised at 29°C on a 14-hr:10-hr light:dark cycle in E3 media as described previously (Burgess and Granato, 2007). All animal protocols were approved by the University of Pennsylvania Institutional Animal Care and Use Committee. See Supplemental Experimental Procedures for further details.

Combined Ca^{2+} and Behavioral Imaging

5-dpf zebrafish larvae were embedded in 2% agarose in glass-bottom petri dishes with tails freed by removing agarose distal to the anus. Drugs were prepared at 100× in DMSO. All images were captured with a Leica CTR7000 HS spinning disc confocal microscope using MetaMorph software (Molecular Devices). Acoustic stimuli were delivered with a Behringer A500 amplifier and Visaton SC 5.9 speaker placed on the microscope stage. High-speed images of tail movement were captured with a Dalsa Genie HM640 camera using

Streampix5 software (Norpix). Latencies and turn angles were manually analyzed. Free-swimming behavioral analysis of CoLo-ablated larvae was done as described previously (Wolman et al., 2011, 2015). See Supplemental Experimental Procedures for further details.

CoLo Interneuron Ablations

Targeted cell ablations were done with a MicroPoint laser (Andor) as described previously (Jain et al., 2014). See Supplemental Experimental Procedures for further details.

Data Analysis

Images were analyzed with Image J (NIH). Statistical analysis was done using Prism 5 (GraphPad), with all data presented as mean ± SEM and p values calculated by two-tailed t tests or one- or two-way ANOVA with post-tests as indicated. See Supplemental Experimental Procedures for further details.

SUPPLEMENTAL INFORMATION

Supplemental Information includes Supplemental Experimental Procedures, three figures, and one movie and can be found with this article online at http://dx.doi.org/10.1016/j.celrep.2015.10.060.

AUTHOR CONTRIBUTIONS

K.C.M. designed and performed all experiments and wrote the manuscript. M.G. designed experiments, supervised the work, and edited the manuscript.

ACKNOWLEDGMENTS

We would like to thank Alberto Pereda and Granato lab members for helpful discussions. K.C.M. was supported by a Ruth L. Kirschstein National Research Service Award (NRSA) F32-NS-077815 from NINDS. M.G. was supported by NIH grants MH103545, MH092257, and EY024861.

Received: May 19, 2015
Revised: September 15, 2015
Accepted: October 20, 2015
Published: November 19, 2015

REFERENCES

Ahrens, M.B., Li, J.M., Orger, M.B., Robson, D.N., Schier, A.F., Engert, F., and Portugues, R. (2012). Brain-wide neuronal dynamics during motor adaptation in zebrafish. Nature *485*, 471–477.

Aljure, E., Day, J.W., and Bennett, M.V. (1980). Postsynaptic depression of Mauthner cell-mediated startle reflex, a possible contributor to habituation. Brain Res. *188*, 261–268.

Bliss, T.V., and Lomo, T. (1973). Long-lasting potentiation of synaptic transmission in the dentate area of the anaesthetized rabbit following stimulation of the perforant path. J. Physiol. *232*, 331–356.

Bristol, A.S., and Carew, T.J. (2005). Differential role of inhibition in habituation of two independent afferent pathways to a common motor output. Learn. Mem. *12*, 52–60.

Broster, B.S., and Rankin, C.H. (1994). Effects of changing interstimulus interval during habituation in Caenorhabditis elegans. Behav. Neurosci. *108*, 1019–1029.

Burgess, H.A., and Granato, M. (2007). Sensorimotor gating in larval zebrafish. J. Neurosci. *27*, 4984–4994.

Carey, R.J., Dai, H., and Gui, J. (1998). Effects of dizocilpine (MK-801) on motor activity and memory. Psychopharmacology (Berl.) *137*, 241–246.

Castellucci, V.F., and Kandel, E.R. (1974). A quantal analysis of the synaptic depression underlying habituation of the gill-withdrawal reflex in Aplysia. Proc. Natl. Acad. Sci. USA *71*, 5004–5008.

Chen, T.-W., Wardill, T.J., Sun, Y., Pulver, S.R., Renninger, S.L., Baohan, A., Schreiter, E.R., Kerr, R.A., Orger, M.B., Jayaraman, V., et al. (2013). Ultrasensitive fluorescent proteins for imaging neuronal activity. Nature *499*, 295–300.

Cichon, J., and Gan, W.-B. (2015). Branch-specific dendritic Ca(2+) spikes cause persistent synaptic plasticity. Nature *520*, 180–185.

Dinstein, I., Heeger, D.J., Lorenzi, L., Minshew, N.J., Malach, R., and Behrmann, M. (2012). Unreliable evoked responses in autism. Neuron *75*, 981–991.

Fischer, T.M., Blazis, D.E., Priver, N.A., and Carew, T.J. (1997). Metaplasticity at identified inhibitory synapses in Aplysia. Nature *389*, 860–865.

Glanzman, D.L. (2009). Habituation in Aplysia: the Cheshire cat of neurobiology. Neurobiol. Learn. Mem. *92*, 147–154.

Groves, P.M., and Thompson, R.F. (1970). Habituation: a dual-process theory. Psychol. Rev. *77*, 419–450.

Halberstadt, A.L., and Geyer, M.A. (2009). Habituation and sensitization of acoustic startle: opposite influences of dopamine D1 and D2-family receptors. Neurobiol. Learn. Mem. *92*, 243–248.

Harvey, C.D., and Svoboda, K. (2007). Locally dynamic synaptic learning rules in pyramidal neuron dendrites. Nature *450*, 1195–1200.

Hebb, D.O. (1964). The Organization of Behaviour, a Neuropsychological Theory (D.O. Hebb).

Jain, R.A., Bell, H., Lim, A., Chien, C.-B., and Granato, M. (2014). Mirror movement-like defects in startle behavior of zebrafish dcc mutants are caused by aberrant midline guidance of identified descending hindbrain neurons. J. Neurosci. *34*, 2898–2909.

Kawakami, K., Abe, G., Asada, T., Asakawa, K., Fukuda, R., Ito, A., Lal, P., Mouri, N., Muto, A., Suster, M.L., et al. (2010). zTrap: zebrafish gene trap and enhancer trap database. BMC Dev. Biol. *10*, 105.

Kimmel, C.B., Patterson, J., and Kimmel, R.O. (1974). The development and behavioral characteristics of the startle response in the zebra fish. Dev. Psychobiol. *7*, 47–60.

Kindt, K.S., Quast, K.B., Giles, A.C., De, S., Hendrey, D., Nicastro, I., Rankin, C.H., and Schafer, W.R. (2007). Dopamine mediates context-dependent modulation of sensory plasticity in C. elegans. Neuron *55*, 662–676.

Kleinhans, N.M., Johnson, L.C., Richards, T., Mahurin, R., Greenson, J., Dawson, G., and Aylward, E. (2009). Reduced neural habituation in the amygdala and social impairments in autism spectrum disorders. Am. J. Psychiatry *166*, 467–475.

Kohashi, T., and Oda, Y. (2008). Initiation of Mauthner- or non-Mauthner-mediated fast escape evoked by different modes of sensory input. J. Neurosci. *28*, 10641–10653.

Korn, H., and Faber, D.S. (2005). The Mauthner cell half a century later: a neurobiological model for decision-making? Neuron *47*, 13–28.

Korn, H., Oda, Y., and Faber, D.S. (1992). Long-term potentiation of inhibitory circuits and synapses in the central nervous system. Proc. Natl. Acad. Sci. USA *89*, 440–443.

Koyama, M., Kinkhabwala, A., Satou, C., Higashijima, S., and Fetcho, J. (2011). Mapping a sensory-motor network onto a structural and functional ground plan in the hindbrain. Proc. Natl. Acad. Sci. USA *108*, 1170–1175.

Krasne, F.B., and Teshiba, T.M. (1995). Habituation of an invertebrate escape reflex due to modulation by higher centers rather than local events. Proc. Natl. Acad. Sci. USA *92*, 3362–3366.

Lacoste, A.M.B., Schoppik, D., Robson, D.N., Haesemeyer, M., Portugues, R., Li, J.M., Randlett, O., Wee, C.L., Engert, F., and Schier, A.F. (2015). A convergent and essential interneuron pathway for Mauthner-cell-mediated escapes. Curr. Biol. *25*, 1526–1534.

Meincke, U., Light, G.A., Geyer, M.A., Braff, D.L., and Gouzoulis-Mayfrank, E. (2004). Sensitization and habituation of the acoustic startle reflex in patients with schizophrenia. Psychiatry Res. *126*, 51–61.

Neumeister, H., Whitaker, K.W., Hofmann, H.A., and Preuss, T. (2010). Social and ecological regulation of a decision-making circuit. J. Neurophysiol. *104*, 3180–3188.

O'Malley, D.M., Kao, Y.H., and Fetcho, J.R. (1996). Imaging the functional organization of zebrafish hindbrain segments during escape behaviors. Neuron *17*, 1145–1155.

Oda, Y., Kawasaki, K., Morita, M., Korn, H., and Matsui, H. (1998). Inhibitory long-term potentiation underlies auditory conditioning of goldfish escape behaviour. Nature *394*, 182–185.

Paranjpe, P., Rodrigues, V., VijayRaghavan, K., and Ramaswami, M. (2012). Gustatory habituation in Drosophila relies on rutabaga (adenylate cyclase)-dependent plasticity of GABAergic inhibitory neurons. Learn. Mem. *19*, 627–635.

Rankin, C.H., Abrams, T., Barry, R.J., Bhatnagar, S., Clayton, D.F., Colombo, J., Coppola, G., Geyer, M.A., Glanzman, D.L., Marsland, S., et al. (2009). Habituation revisited: an updated and revised description of the behavioral characteristics of habituation. Neurobiol. Learn. Mem. *92*, 135–138.

Roberts, A.C., Reichl, J., Song, M.Y., Dearinger, A.D., Moridzadeh, N., Lu, E.D., Pearce, K., Esdin, J., and Glanzman, D.L. (2011). Habituation of the C-start response in larval zebrafish exhibits several distinct phases and sensitivity to NMDA receptor blockade. PLoS ONE *6*, e29132.

Satou, C., Kimura, Y., Kohashi, T., Horikawa, K., Takeda, H., Oda, Y., and Higashijima, S. (2009). Functional role of a specialized class of spinal commissural inhibitory neurons during fast escapes in zebrafish. J. Neurosci. *29*, 6780–6793.

Scott, E.K., Mason, L., Arrenberg, A.B., Ziv, L., Gosse, N.J., Xiao, T., Chi, N.C., Asakawa, K., Kawakami, K., and Baier, H. (2007). Targeting neural circuitry in zebrafish using GAL4 enhancer trapping. Nat. Methods *4*, 323–326.

Shirinyan, D., Teshiba, T., Taylor, K., O'Neill, P., Lee, S.C., and Krasne, F.B. (2006). Rostral ganglia are required for induction but not expression of crayfish escape reflex habituation: role of higher centers in reprogramming low-level circuits. J. Neurophysiol. *95*, 2721–2724.

Simons-Weidenmaier, N.S., Weber, M., Plappert, C.F., Pilz, P.K.D., and Schmid, S. (2006). Synaptic depression and short-term habituation are located in the sensory part of the mammalian startle pathway. BMC Neurosci. *7*, 38.

Swerdlow, N.R., Light, G.A., Cadenhead, K.S., Sprock, J., Hsieh, M.H., and Braff, D.L. (2006). Startle gating deficits in a large cohort of patients with schizophrenia: relationship to medications, symptoms, neurocognition, and level of function. Arch. Gen. Psychiatry *63*, 1325–1335.

Takahashi, M., Narushima, M., and Oda, Y. (2002). In vivo imaging of functional inhibitory networks on the mauthner cell of larval zebrafish. J. Neurosci. *22*, 3929–3938.

Thermes, V., Grabher, C., Ristoratore, F., Bourrat, F., Choulika, A., Wittbrodt, J., and Joly, J.-S. (2002). I-SceI meganuclease mediates highly efficient transgenesis in fish. Mech. Dev. *118*, 91–98.

Thompson, R.F., and Spencer, W.A. (1966). Habituation: a model phenomenon for the study of neuronal substrates of behavior. Psychol. Rev. *73*, 16–43.

Weber, M., Schnitzler, H.-U., and Schmid, S. (2002). Synaptic plasticity in the acoustic startle pathway: the neuronal basis for short-term habituation? Eur. J. Neurosci. *16*, 1325–1332.

Weiss, S.A., Preuss, T., and Faber, D.S. (2008). A role of electrical inhibition in sensorimotor integration. Proc. Natl. Acad. Sci. USA *105*, 18047–18052.

Wen, J.A., and Barth, A.L. (2011). Input-specific critical periods for experience-dependent plasticity in layer 2/3 pyramidal neurons. J. Neurosci. *31*, 4456–4465.

Wicks, S.R., and Rankin, C.H. (1996). Recovery from habituation in Caenorhabditis elegans is dependent on interstimulus interval and not habituation kinetics. Behav. Neurosci. *110*, 840–844.

Wolman, M.A., Jain, R.A., Liss, L., and Granato, M. (2011). Chemical modulation of memory formation in larval zebrafish. Proc. Natl. Acad. Sci. USA *108*, 15468–15473.

Wolman, M.A., de Groh, E.D., McBride, S.M., Jongens, T.A., Granato, M., and Epstein, J.A. (2014). Modulation of cAMP and ras signaling pathways improves distinct behavioral deficits in a zebrafish model of neurofibromatosis type 1. Cell Rep. *8*, 1265–1270.

Wolman, M.A., Jain, R.A., Marsden, K.C., Bell, H., Skinner, J., Hayer, K.E., Hogenesch, J.B., and Granato, M. (2015). A genome-wide screen identifies PAPP-AA-mediated IGFR signaling as a novel regulator of habituation learning. Neuron *85*, 1200–1211.

Yamanaka, I., Miki, M., Asakawa, K., Kawakami, K., Oda, Y., and Hirata, H. (2013). Glycinergic transmission and postsynaptic activation of CaMKII are required for glycine receptor clustering in vivo. Genes Cells *18*, 211–224.

Yao, C., Vanderpool, K.G., Delfiner, M., Eddy, V., Lucaci, A.G., Soto-Riveros, C., Yasumura, T., Rash, J.E., and Pereda, A.E. (2014). Electrical synaptic transmission in developing zebrafish: properties and molecular composition of gap junctions at a central auditory synapse. J. Neurophysiol. *112*, 2102–2113.

Cell Reports

Supplemental Information

In Vivo Ca^{2+} Imaging Reveals that Decreased Dendritic Excitability Drives Startle Habituation

Kurt C. Marsden and Michael Granato

Supplemental Data

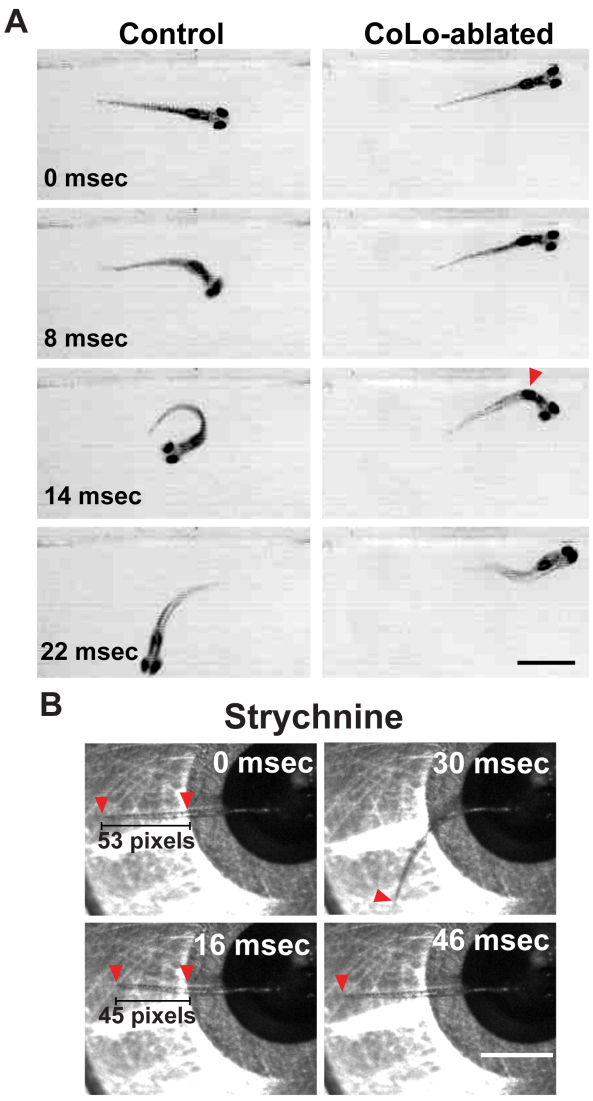

Figure S1. CoLo ablation and strychnine treatment cause abnormal startle responses, Related to Figures 3 and 4. (A) Free-swimming control larvae perform normal startle responses to acoustic stimulation while CoLo-ablated larvae respond at normal latency but with altered kinematics. The tail caudal to the CoLo ablations (red arrowhead) straightens rather than contracting on one side (scale bar 10 μm). **(B)** Representative example of abnormal startle after 100 μM strychnine treatment in head-restrained larvae. Movement initiates at 8 ms (not shown), and the tail straightens and shortens (16 ms, indicated by red arrowheads), followed by a normal counterbend (30 ms) and relaxation (46 ms).

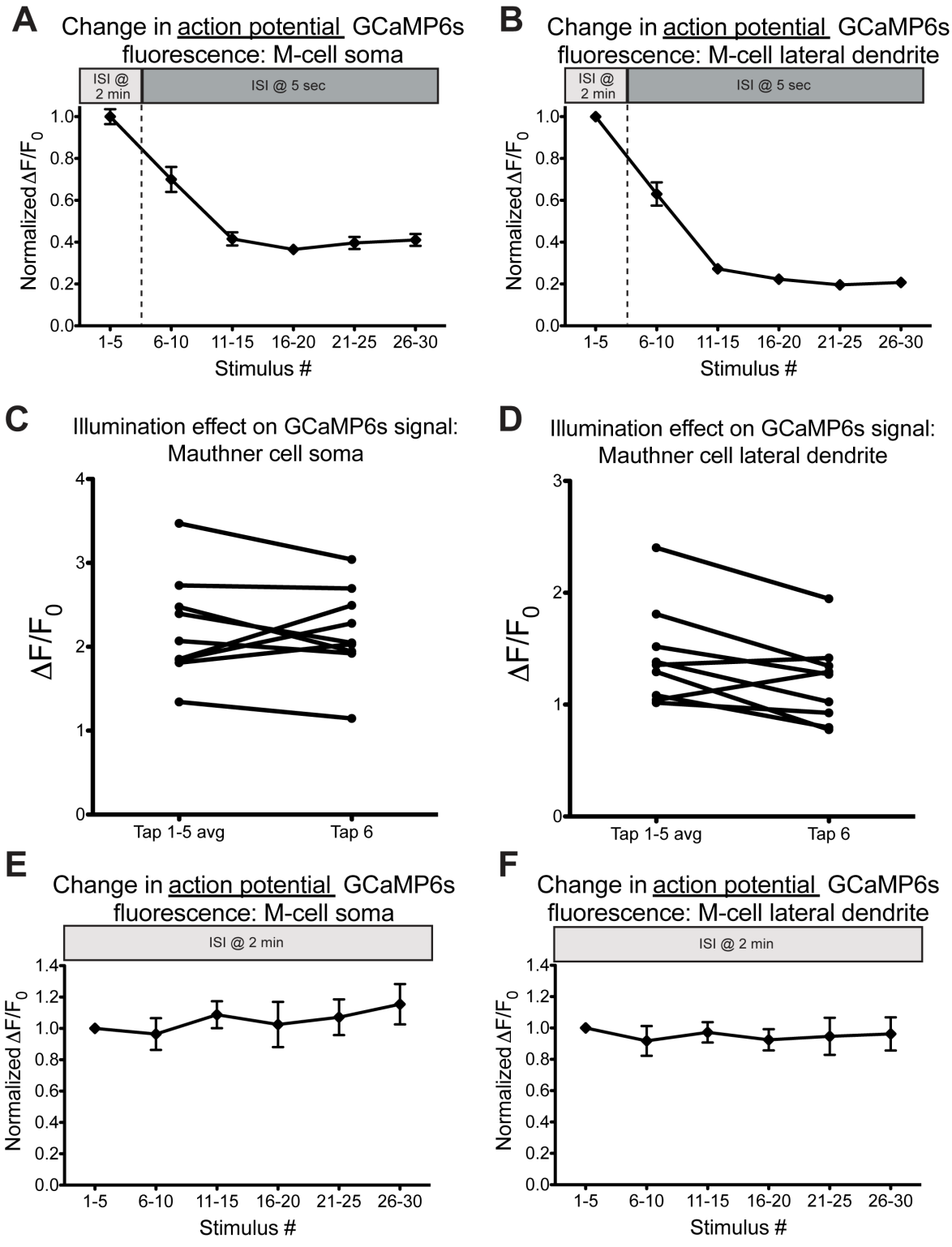

Figure S2. Repeated stimulation reduces GCaMP6s fluorescence, Related to Figure 4. (A) Peak M-cell somatic $\Delta F/F_0$ values were averaged for 5 strong, startle-inducing stimuli with a 2 min inter-stimulus interval (ISI; Tap 1-5 avg) followed by 3

minutes of laser illumination without acoustic stimulation, followed by one additional acoustic stimulus (Tap 6) to measure the effect of sustained laser illumination on peak $\Delta F/F_0$. Somatic signals did nto significantly change on average (0.13 ± 6.45%; n=9). Each dot represents an individual fish. **(B)** Peak M-cell lateral dendrite $\Delta F/F_0$ values during the same assay are decreased by 14.8 ± 6.41% (n = 9). **(C)** The effect of repeated stimulation on peak $\Delta F/F_0$ signals in the M-cell soma during the 30-stimulus habituation assay. Plotted are peak M-cell somatic $\Delta F/F_0$ values ***only*** for action potential-like events in which there was a startle response ***and*** a strong Ca^{2+} signal in the M-cell soma (>10 SDs above signals when there was no startle response). These signals were significantly reduced relative to the first 5 non-habituating stimuli (58.9 ± 2.84%; n = 26 fish). **(D)** The change in lateral dendrite $\Delta F/F_0$ during the same action-potential-like events plotted in (C). These signals were significantly reduced relative to the first 5 non-habituating stimuli (79.3 ± 1.44%; n = 26 fish). (**E**) The change in M-cell soma $\Delta F/F_0$ over 30 stimuli with a 2 min ISI. These signals showed no significant change (15.4 ± 12.9%; n = 5 fish). (**F**) The change in M-cell lateral dendrite $\Delta F/F_0$ during the same 30-stimulus, 2 min ISI protocol in (E). These signals showed no significant change (3.8 ± 10.6%; n = 5 fish).

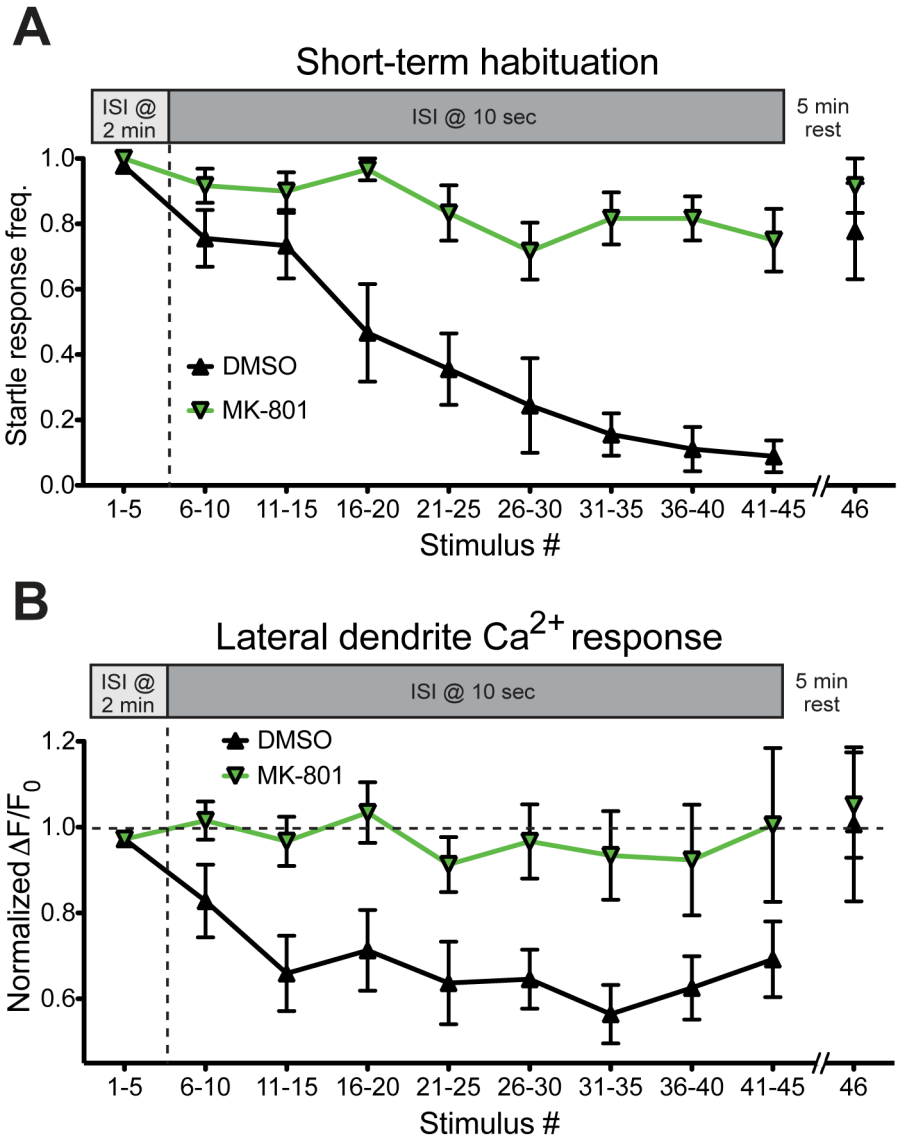

Supplemental Figure 3. Increasing inter-stimulus interval does not change the mechanism of short-term acoustic startle habituation, Related to Figure 4.

(A) 45-stimulus protocol with 10 s ISI induces habituation in DMSO but not MK-801-treated fish. Startle responsiveness recovers after 5 min rest. **(B)** Normalized Lateral dendrite Ca^{2+} responses are significantly depressed in DMSO (n = 6) vs. MK-801-treated (n = 8) fish ($p < 0.0001$, 2-way ANOVA). Peak fluorescence recovers after 5 min rest.

Movie S1. Increasing acoustic stimulus intensity increases lateral dendrite Ca^{2+} responses, Related to Figure 2. A series of 6 acoustic stimuli of increasing intensity were presented to a head-restrained larva. This representative movie shows that GCaMP6s signals in the Mauthner cell lateral dendrite increase with increasing stimulus intensity (indicated by speaker size). Somatic activity is only detected when the larva performs a startle response.

Supplemental Experimental Procedures

Generation of Gal4FF-62a;UAS:GCaMP6s *transgenic line*

pCMV-GCaMP6s was purchased from Addgene (Chen et al., 2013), and GCaMP6s was cloned into a pENTR Gateway (Invitrogen) cloning vector using *BglII/BamHI* and *XbaI* restriction sites. Using LR2+ clonase (Invitrogen) GCaMP6s was then inserted into a pDEST Gateway expression vector containing flanking I-SceI sites and *cmlc2:EGFP* on the reverse strand for labeling of cardiac muscle. I-SceI-mediated transgenesis was performed as described previously (Thermes et al., 2002), and the *UAS:GCaMP6s;cmlc2:EGFP* line was generated in the Tüpfel longfin (TLF) strain. *Gal4FF-62A* fish were kindly provided by Koichi Kawakami (Kawakami et al., 2010; Yamanaka et al., 2013).

Combined Ca^{2+} and behavioral imaging

All procedures were done at room temperature (~22ºC). For imaging head-restrained larvae, agarose was dissolved at 2% in bath solution containing (in mM): 112 NaCl, 5 HEPES pH 7.5, 2 $CaCl_2$, 3 glucose, 2 KCl, 1 $MgCl_2$ (Ikeda et al., 2013). MK-801

(M107; Sigma-Aldrich) and strychnine (S-0532; Sigma-Aldrich) were prepared at 100X in DMSO and diluted to 500 and 100 μM, respectively, in bath solution. DMSO (1% in bath solution), MK-801 and strychnine treatments were applied to mounted larvae for 15 minutes prior to imaging and remained throughout the duration of testing.

Confocal images were captured with a Leica CTR7000 HS microscope equipped with a Yokogawa CSU-X1 spinning disc and Andor iXon EMCCD camera. Focusing on the brightest plane in the sample, a single plane was captured for each timepoint at 512x512 pixel resolution with no signal summation and little or no movement of the sample during stimulation. All acoustic stimuli were 3 ms duration sinusoids with 1000 Hz frequency and variable intensity. Stimulus intensities were calibrated using a PCB Piezotronics accelerometer (model #355B04) and signal conditioner (#482A21), with voltage outputs read by an oscilloscope and converted to dB using the formula dB = 20 log (V / 0.775). The dB scale is based on human hearing, so negative dB values reflect sounds below the human detection threshold that may still be detectable by other species.

An infrared LED array was placed above the stage to illuminate the sample for high-speed behavior imaging with a Dalsa Genie HM640 camera fitted with an infrared bandpass filter. Precise timing and triggering of the acoustic stimulus, high-speed camera and confocal microscope were achieved using a National Instruments Data Acquisition device (NI-USB 6259).

CoLo interneuron ablations

At 2-2.5 dpf, embryos carrying 1 or 2 copies of the Tol056 GFP enhancer trap transgene that labels CoLos and M-cells (Satou et al., 2009) were mounted in 1.2%

agarose. CoLos on both sides of the spinal cord caudal to the 5th segment were ablated with a MicroPoint ablation system (Andor Technology) consisting of a nitrogen-pumped dye laser (wavelength 435 nm) controlled by Slidebook (version 6.0) on a spinning disc confocal microscope (Olympus). Larvae recovered for 24 hrs in E3 and ablations were verified by imaging. Only individuals with complete, unambiguous loss of CoLos were analyzed. Control larvae were mounted, imaged and handled in the same manner without laser ablation. Larvae recovered for an additional 12-24 hrs post-imaging in E3 prior to behavioral testing at 5 dpf.

Data analysis

Using Image J (NIH), background fluorescence was removed by subtracting pixels below the mode value of each image. Regions of interest (ROIs) were manually selected for each timelapse as in Figure 3A while blinded to the treatment condition. Fluorescence intensity values were calculated by dividing integrated pixel value by ROI area. F_0 values represent the mean fluorescence intensity in each ROI for the 20 timepoints (1 sec) immediately prior to each acoustic stimulus. For M-cell somatic firing frequency analysis (Figure 3C) 'firing' was defined as a $\Delta F/F_0 > 10$ standard deviations above the mean $\Delta F/F_0$ for events with no behavioral response. For lateral dendrite analysis during habituation (Figure 4D), $\Delta F/F_0$ values were normalized to the curve of the change in action potential-associated lateral dendrite activity (Supplementary Figure 2D). Rise times and decay times were obtained by single exponential growth and decay fits, respectively, using Prism 5 software (GraphPad).

Supplemental References

Chen, T.-W., Wardill, T. J., Sun, Y., Pulver, S. R., Renninger, S. L., Baohan, A., et al. (2013). Ultrasensitive fluorescent proteins for imaging neuronal activity. *Nature*, *499*(7458), 295–300. http://doi.org/10.1038/nature12354

Ikeda, H., Delargy, A. H., Yokogawa, T., Urban, J. M., Burgess, H. A., & Ono, F. (2013). Intrinsic properties of larval zebrafish neurons in ethanol. *PLoS ONE*, *8*(5), e63318. http://doi.org/10.1371/journal.pone.0063318

Kawakami, K., Abe, G., Asada, T., Asakawa, K., Fukuda, R., Ito, A., et al. (2010). zTrap: zebrafish gene trap and enhancer trap database. *BMC Developmental Biology*, *10*(1), 105. http://doi.org/10.1186/1471-213X-10-105

Satou, C., Kimura, Y., Kohashi, T., Horikawa, K., Takeda, H., Oda, Y., & Higashijima, S. I. (2009). Functional Role of a Specialized Class of Spinal Commissural Inhibitory Neurons during Fast Escapes in Zebrafish. *The Journal of Neuroscience : the Official Journal of the Society for Neuroscience*, *29*(21), 6780–6793. http://doi.org/10.1523/JNEUROSCI.0801-09.2009

Thermes, V., Grabher, C., Ristoratore, F., Bourrat, F., Choulika, A., Wittbrodt, J., & Joly, J.-S. (2002). I-SceI meganuclease mediates highly efficient transgenesis in fish. *Mechanisms of Development*, *118*(1-2), 91–98.

Yamanaka, I., Miki, M., Asakawa, K., Kawakami, K., Oda, Y., & Hirata, H. (2013). Glycinergic transmission and postsynaptic activation of CaMKII are required for glycine receptor clustering in vivo. *Genes to Cells : Devoted to Molecular & Cellular Mechanisms*, *18*(3), 211–224. http://doi.org/10.1111/gtc.12032